ChemComm

ROYAL SOCIETY OF CHEMISTRY

COMMUNICATION

View Article Online
View Journal | View Issue

Published on 29 July 2020. Downloaded by Ohio State University Libraries on 4/30/2021 7:47:30 PM.

Check for updates

Cite this: *Chem. Commun.*, 2020, **56**, 10337

Received 17th May 2020,
Accepted 29th July 2020

DOI: 10.1039/d0cc03528a

rsc.li/chemcomm

Self-assembly of a robust, reduction-sensitive camptothecin nanotube†

Yuan Sun, Cathleen M. Fry, Aileen Shieh and Jon R. Parquette *

The self-assembly and covalent crosslinking of a camptothecin (CPT) tetrapeptide nanotube is reported. Intermolecular disulfide bond formation of a self-assembled CPT-peptide reversibly stabilized the nanotubes toward dissociation at low concentrations, resulting in inhibited release of CPT. In the presence of dithiothreitol (DTT), the release of CPT was significantly accelerated. The crosslinked nanotubes also exhibited *in vitro* cytotoxicity against human non-small cell lung cancer cell lines A549 and H460.

The application of nanotechnology to the delivery of therapeutic agents offers a tremendous potential to reduce side effects and increase the efficacy of treatment.[1] Self-assembly is a powerful method to construct well-defined nanomaterials from simple building blocks.[2,3] Nanoscale drug formulations created by self-assembly allow the drug to serve as its own carrier and generally produces higher drug loading levels than methods using excipient carriers.[4] This approach relies on amphiphilic drug conjugates to assemble into nanostructured vehicles *via* noncovalent interactions, above a critical assembly concentration.[5,6] To achieve optimal therapeutic efficacy, drug delivery systems must remain stable under extracellular conditions but rapidly release the drug payload after entering tumor cells.[7] In contrast to nanomedicines created by covalent attachment to excipient carriers, the nanostructure of self-assembled systems depends on environmental conditions and are often in equilibrium with unassembled monomers. This approach produces single-component nanomedicines with enhanced properties, such as an ability to passively accumulate in tumor tissues, longer circulation times, and protection from degradation.[8] However, the noncovalent assembly process is often limited by premature disassembly and release of the drug prior to reaching the targeted site.

The self-assembly of small molecules derivatized with bioactive components is well suited as a strategy to efficiently create drug delivery vehicles with nanometer dimensions and enhanced properties.[9] Common organic building blocks for self-assembled materials are amphiphilic polymers and small molecules,[10,11] among which amphiphilic peptides are of special interest due to their low toxicity and well-tolerated biocompatibility.[12–16] The utility of noncovalent nanostructures for drug delivery applications benefits from the enhanced permeability and retention (EPR) effect, which allows the nanoscale materials to be delivered selectively into tumor cells.[17] However, efficacy and safety requires that the nanostructures remain intact at therapeutically relevant concentrations and that release of the drug occur only at the target site.[18–20] To address these issues, stimuli-responsive carriers have been developed that are stable under extracellular conditions, but rapidly release the drug payload upon a change in local environment, resulting in increased efficacy, reduced side effects and lower toxicity.[21–24] Systems that respond to stimuli such as pH, temperature, ionic strength, and light, have been investigated for cancer therapy.[25–29] One strategy for triggered drug release relies on a disulfide bond as a prodrug linkage,[6,30–35] due to the potential to release the drug in the presence of endogenous reducing agents, such as glutathione (GSH) and thioredoxin (Trx), which are overexpressed in cancer cells.[36–38] Importantly, these are present in blood and normal extracellular matrices at significantly lower concentrations than in the cytosol and the nucleus, which maintain a high redox potential.[39] Thus, disulfide bonds are generally stable under extracellular conditions in the circulation, but are cleaved upon entering the cellular environment.

Previously, we reported that camptothecin and 5-fluorouracil–peptide conjugates efficiently self-assemble into well-defined nanotubes,[14–16] which exhibited high cytotoxicity against several cancer cell lines. The assembled CPT-peptide nanotubes protected the drug from deactivation *via* hydrolytic ring-opening of the active lactone form in PBS and serum. Similarly, the release rate of the drug, which occurs *via* cleavage of the 20-*O*-succinyl linkage,[40] was significantly reduced because the nanotube assembly process sequesters the CPT-molecules within the hydrophobic walls of the nanotube, thereby isolating

Department of Chemistry and Biochemistry, The Ohio State University, 100 W. 18th Ave., Columbus, Ohio 43210, USA. E-mail: parquett@chemistry.ohio-state.edu; Fax: +1 614 292 1685

† Electronic supplementary information (ESI) available. See DOI: 10.1039/d0cc03528a

Published on 29 July 2020. Downloaded by Ohio State University Libraries on 4/30/2021 7:47:30 PM.

the drug from the aqueous interface. The rate of drug release in these systems was highly dependent on concentration, due to shifts in the position of the nanotube-monomer equilibrium. Therefore, the structural integrity of the nanotubes would potentially be compromised at therapeutically relevant, micromolar concentrations. Based on the potential for disulfide crosslinking to stabilize the nanotube structure,[41,42] we reasoned that oxidative crosslinking would also prevent hydrolytic drug release at low concentrations in the absence of the intracellular reducing environment. In this work, we report the self-assembly and oxidative crosslinking of a CPT-tetrapeptide (**A**, CPT-CCKK) nanotube as a strategy to control the nanostructure stability and CPT release rate. Reduction of the disulfide crosslinks reinstates the monomer-nanotube equilibrium, resulting in rapid hydrolytic release of the CPT. The crosslinked nanotubes exhibited *in vitro* cytotoxicity against human non-small cell lung cancer cell lines.

The design of CPT-peptide **A** (CPT-CCKK) was based on our previously reported dilysine-CPT peptides, which assembled into nanotubes *via* a combination of β-sheet interactions and hydrophobic sequestration of the CPT segment.[14–16] In this design, the lysine side-chains provided the solubility and amphiphilicity required to drive self-assembly in water (Fig. 1). The CPT molecule was appended to the α-amino group of the N-terminal lysine residue *via* a 20-*O*-succinyl linkage, which would release active CPT upon hydrolytic cleavage.[43] In order to confer amphiphilicity to the peptide, two cysteine residues were positioned between the lysine and CPT moieties. The peptide was prepared using standard Fmoc/*t*-Boc solid-phase peptide synthesis, followed by on-resin amidation of the N-terminal cysteine residue with 20-*O*-camptothecin succinic acid.

The self-assembly of **A** was explored by transmission electron microscopy (TEM) and UV-vis/CD spectroscopy. A sample of **A**, incubated at 20 mM in PBS for 72 h, then diluted to 1 mM, exhibited an array of nanotubes displaying a wide range of diameters (~232 ± 60 nm) and lengths of several micrometers

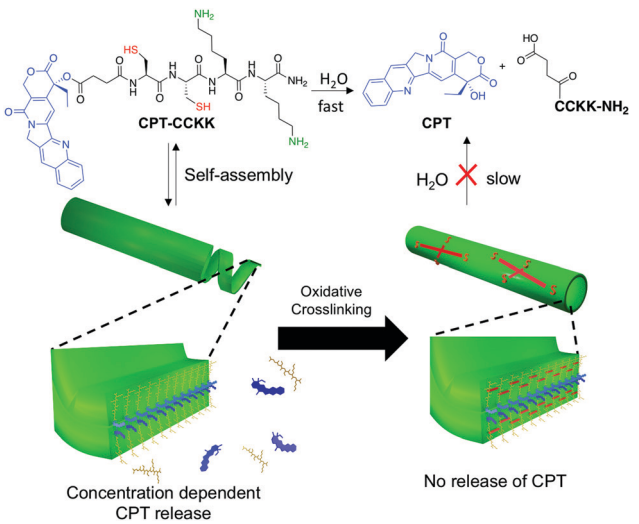

Fig. 1 Structural design of CPT-CCKK peptide, **A**, and crosslinking *via* disulfide bond formation between cysteines.

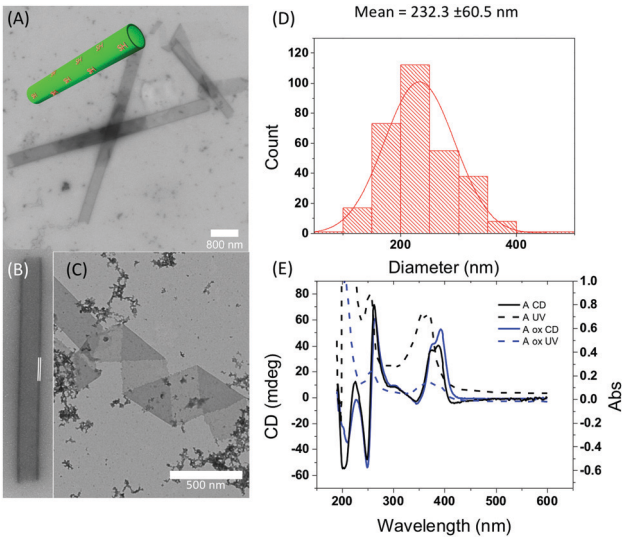

Fig. 2 TEM images of **A** in PBS (3 days, pH 7.4, 20 mM), showing (a) mature nanotubes; (b) wall thickness of nanotubes; (c) coiled ribbon intermediates formed after 24 h in PBS (10 mM); and (d) histograms of nanotube diameter distributions, extracted from TEM images. (e) Circular dichroic (CD) and ultraviolet (UV-vis) spectra of assembled **A** (black) and after oxidation (blue). Samples were prepared by dissolving **A** in PBS (20 mM, 3 days), diluting to 0.25 mM for CD/UV and, for TEM, to 1 mM prior to imaging using a carbon coated copper grid and negatively stained with 2% wt uranyl acetate. **A-ox** samples were obtained by oxidation with 10% v/v DMSO, pelleting at 80 000 rpm (278 835 g) for 1 h and resuspension in PBS.

by TEM imaging (Fig. 2a and d). At lower concentrations in PBS (0.2 mM), nanotubes were not formed (Fig. S1, ESI†). The lower solubility of the peptide in water required the nanotubes to be assembled at a lower concentration (10 mM). Under these conditions, the nanotubes exhibited diameters of ~135 nm, but were significantly shorter and less mature (Fig. S14 and S15, ESI†). The enhanced self-assembly in PBS, compared with pure water, was likely driven by the presence of salts that screen the positive charges of the lysine side-chains, which reduced interpeptide, electrostatic repulsions.[44] The UV-vis spectrum revealed bands at 350 and 368 nm in PBS that were only slightly red-shifted relative to spectra in 2,2,2-trifluoroethanol (TFE), in which the peptide remained in a monomeric state (Fig. 2e and Fig. S11, ESI†). Red-shifting of UV bands are usually indicative of the presence of J-type π–π interactions within an aggregate.[45] The small red-shift, in conjunction with the CD signal intensity in the region of the CPT absorption (330–400 nm), indicated that the CPT moiety contributes hydrophobic effects, rather than extensive π–π interactions to the assembly process. TEM images of samples at earlier stages of assembly (after aging 24 h at 10 mM) showed mature nanotubes along with helically coiled ribbons (Fig. 2c). The presence of these intermediates, along with helical striations on mature nanotubes (Fig. 2a and Fig. S14, ESI†), suggest that the nanotubes emerged from ribbons that progressively coiled into helical ribbons, which then laterally merged into the final nanotube structure. The thickness of the nanotube walls (5.98 ± 1.2 nm), as measured by TEM imaging (Fig. 2b, inset and Fig. S18, ESI†), indicated a bilayer wall structure based on the extended length of **A**

 This journal is © The Royal Society of Chemistry 2020

Published on 29 July 2020. Downloaded by Ohio State University Libraries on 4/30/2021 7:47:30 PM.

(~2.7 nm) (Fig. S7, ESI†). Fourier-transform infrared (FTIR) spectra of **A**, prepared in PBS (20 mM, D_2O) did not show amide I bands characteristic of β-sheet secondary structure (Fig. S12, ESI†).[46] However, the presence of a large band at 1643 cm^{-1} in the deconvoluted spectra indicated that **A** existed entirely in a random coil conformation.[47] This information, along with the CD spectra, indicated that the nanotubes were formed by amphiphilic self-asssembly rather than β-sheet hydrogen-bonding or π–π interactions.

We reasoned that crosslinking the nanotubes, *via* oxidative disulfide bond formation, would enhance their structural integrity under adverse conditions such as changes in environment or concentration. Covalent capture of the nanotubes would also be expected to hamper the hydrolytic release of CPT by preventing dissociation of the nanotube into monomer. This strategy has been shown to reversibly rigidify hydrogels and peptide nanofibers.[41,48] Accordingly, after self-assembly of the nanotubes in PBS at 20 mM, the cysteine thiols were oxidized by exposing the solution to 10% DMSO for 72 h, monitoring the process using Ellman's reagent (5,5′-dithiobis-(2-nitrobenzoic acid)) (DTNB) (Fig. 3b and Fig. S2, ESI†).[49] The oxidation produced nanotubes that were similar in morphology and diameter, but also caused some inter-nanotube crosslinking, as evidenced by the presence of some bundling (Fig. 3a). The robustness of the crosslinked nanotubes was investigated by using ultracentrifugation to pellet the nanotubes, followed by resuspension in TFE, in which the uncrosslinked nanotubes readily dissociated into monomers. Accordingly, dissolving uncrosslinked **A** in TFE at 10 mM did not result in the formation of nanotubes that were observable by TEM imaging (Fig. S16a, ESI†). In contrast, images of the crosslinked nanotubes (**A-ox**), after resuspension in TFE for 72 h, showed the presence of intact nanotubes (Fig. S16b, ESI†).

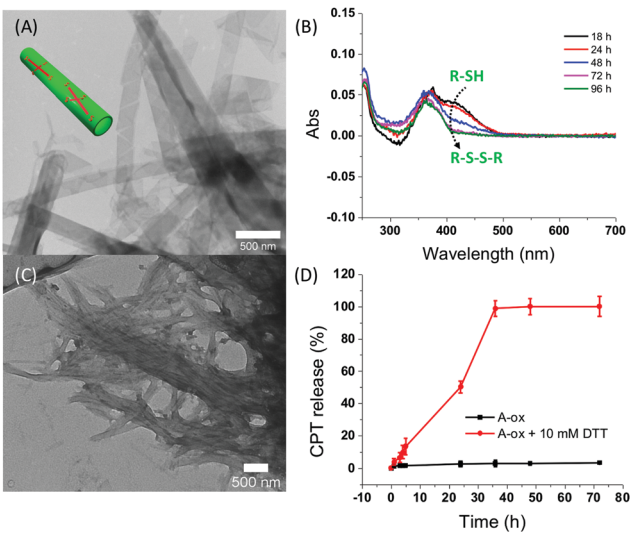

Fig. 3 (a) TEM image of **A**, assembled in PBS (pH 7.4, 20 mM), after oxidization with 10% DMSO v/v for 72 h. (b) Time dependence of the oxidation of assembled **A** with DMSO, as monitored by reaction with DTMB (Ellman's test). The decrease in the 415 nm absorption over time indicates the consumption of free thiols in the sample. (c) TEM of crosslinked nanotubes of **A** (PBS, 10 mM, 3 days) after pelleting by ultracentrifuge and resuspension in TFE (1 mM). (d) Release of CPT, as monitored by HPLC, from crosslinked nanotubes of **A** (100 μM in PBS at 37.5 °C) in presence and absence of dithiothreitol (DTT).

Previously, we observed that nanotube assembly at higher concentrations impeded hydrolytic drug release.[14–16] At lower concentrations, a shift in the monomer-nanotube equilibrium toward monomer significantly accelerated release of the drug. Based on those studies, the self-assembly of **A** into nanotubes would be expected to sequester the hydrophobic CPT structure within the hydrophobic nanotube walls, thereby protecting the 20-*O*-succinyl linkage from the hydrolytic aqueous environment. The rate of hydrolytic release of CPT from the crosslinked nanotubes of **A** was measured at 37.5 °C in PBS at 100 μM by HPLC in the reduced and crosslinked states (Fig. 3d). After 72 h, less than 10% of the CPT was released from the crosslinked nanotubes. In contrast, when the crosslinked nanotubes were exposed to 10 mM dithiothreitol (DTT), complete release of CPT occurred within ~35 h (Fig. 3d and Fig. S4–S7, ESI†), at a similar rate to the parent, uncrosslinked nanotubes at 100 μM. In the crosslinked state, the nanotube structure was stable even at 100 μM, a concentration that would induce dissociation of the uncrosslinked nanotubes.[16] Thus, the release rate was responsive to the position of the nanotube-monomer equilibrium. Oxidative crosslinking rendered the nanotubes insensitive to concentration, resulting in protection of the CPT linkage from the hydrolytic aqueous interface. When the disulfide crosslinks were reduced by DTT, the equilibrium shifted toward monomeric **A**, which experienced rapid hydrolysis of the CPT peptide linkage.

To evaluate the potential for the crosslinked nanotubes of **A** to release CPT, we assessed the cytotoxic efficacy against human non-small cell lung cancer (NSCLC) cell lines A549 and H460. The cytotoxic activity was assayed using an MTT-assay over the course of a 96 h incubation period, resulting in IC_{50} values of 0.22 μM and 0.28 μM, for the unoxidized nanotubes of **A**, and 0.20 μM and 0.27 μM for CPT, respectively (Fig. 4a). These values reflect a comparable cytotoxicity with parental CPT for cells lines A549 and H460. The lower cytotoxicity of **A**, compared with CPT, can be attributed to the time-dependent hydrolytic release of CPT from **A**. In contrast, the crosslinked nanotubes (**A-ox**) exhibited lower cytotoxicity against the A549 compared with the H460 cell line (Fig. 4b). For example, **A-ox** displayed IC_{50} values of 2.43 and 0.21 μM against the A549 and H460 cell lines, respectively. The differential cytotoxicity toward these two cell lines likely emanates from the need for intracellular reduction of the disulfide to produce active CPT. The glutathione concentration in H460 cells has been reported to be twice that of the A549 cell line, which would lead to faster CPT release.[50,51]

In summary, we have reported the self-assembly and oxidative crosslinking of a CPT-peptide nanotube. Incorporation of two cysteine residues within the peptide sequence allowed for covalent casting of the nanotubes to be achieved *via* oxidative disulfide bond formation. Reversible crosslinking by oxidation/reduction increases or decreases the nanotube stability, relative

Published on 29 July 2020. Downloaded by Ohio State University Libraries on 4/30/2021 7:47:30 PM.

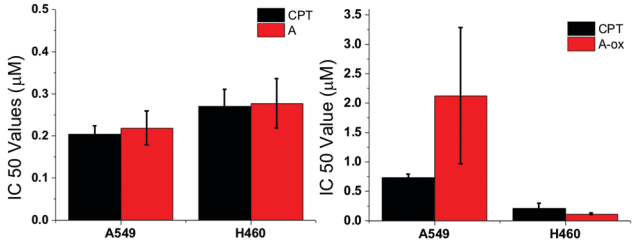

Fig. 4 (a) Cytotoxicity of non-crosslinked nanotube **A** and CPT against human non-small cell lung cancer (NSCLC) cell lines A549 and H460; (b) cytotoxicity of crosslinked nanotube **A** and CPT against A549 and H460.

to the CPT-peptide monomer. The crosslinked nanotubes did not produce CPT at a significant rate; whereas, reduction of the disulfide crosslinks triggered rapid hydrolytic release of the drug. The crosslinked nanotubes displayed cytotoxicity against both A549 and H460 cancer cell lines. However, the nanotubes exhibited significantly greater cytotoxicity toward the H460 cells, which maintained a 2-fold higher GSH concentration. The ability to modulate the integrity of the nanotubes and the corresponding rate of CPT production *via* reversible crosslinking will enable the design of more selective delivery vehicles for anticancer chemotherapeutic agents.

This work was supported by the National Science Foundation (CHE-1708390) and Center for Applied Plant Sciences (CAPS) of the Ohio State University. We acknowledge the technical assistance and usage of the Campus Microscopy & Imaging Facility at OSU.

Conflicts of interest

There are no conflicts to declare.

Notes and references

1 J. Liu, R. Zhang and Z. P. Xu, *Small*, 2019, **15**, 1900262.
2 G. M. Whitesides and B. Grzybowski, *Science*, 2002, **295**, 2418–2421.
3 S. H. Kim and J. R. Parquette, *Nanoscale*, 2012, **4**, 6940–6947.
4 H. Cui and B. Xu, *Chem. Soc. Rev.*, 2017, **46**, 6430–6432.
5 A. G. Cheetham, R. W. Chakroun, W. Ma and H. Cui, *Chem. Soc. Rev.*, 2017, **46**, 6638–6663.
6 P. Schiapparelli, P. Zhang, M. Lara-Velazquez, H. Guerrero-Cazares, R. Lin, H. Su, R. W. Chakroun, M. Tusa, A. Quinones-Hinojosa and H. Cui, *J. Controlled Release*, 2020, **319**, 311–321.
7 S. Kim, Y. Shi, J. Y. Kim, K. Park and J.-X. Cheng, *Expert Opin. Drug Delivery*, 2010, **7**, 49–62.
8 Z. Li, C. Xiao, T. Yong, Z. Li, L. Gan and X. Yang, *Chem. Soc. Rev.*, 2020, **49**, 2273–2290.
9 I. W. Hamley, *Chem. Rev.*, 2017, **117**, 14015–14041.
10 A. G. Cheetham, P. Zhang, Y.-A. Lin, L. L. Lock and H. Cui, *J. Am. Chem. Soc.*, 2013, **135**, 2907.
11 J. Zhou, J. Li, X. Du and B. Xu, *Biomaterials*, 2017, **129**, 1–27.
12 H. Su, P. Zhang, A. G. Cheetham, J. M. Koo, R. Lin, A. Masood, P. Schiapparelli, A. Quinones-Hinojosa and H. Cui, *Theranostics*, 2016, **6**, 1065–1074.
13 Y. Wang, A. G. Cheetham, G. Angacian, H. Su, L. Xie and H. Cui, *Adv. Drug Delivery Rev.*, 2017, **110–111**, 112–126.
14 Y. Sun, A. Shieh, S. H. Kim, S. King, A. Kim, H.-L. Sun, C. M. Croce and J. R. Parquette, *Bioorg. Med. Chem. Lett.*, 2016, **26**, 2834–2838.
15 Y. Sun, J. A. Kaplan, A. Shieh, H.-L. Sun, C. M. Croce, M. W. Grinstaff and J. R. Parquette, *Chem. Commun.*, 2016, **52**, 5254–5257.
16 S. H. Kim, J. A. Kaplan, Y. Sun, A. Shieh, H. L. Sun, C. M. Croce, M. W. Grinstaff and J. R. Parquette, *Chem. – Eur. J.*, 2015, **21**, 101–105.
17 H. Maeda, J. Wu, T. Sawa, Y. Matsumura and K. Hori, *J. Controlled Release*, 2000, **65**, 271–284.
18 O. C. Farokhzad and R. Langer, *ACS Nano*, 2009, **3**, 16–20.
19 X. Huang and C. S. Brazel, *J. Controlled Release*, 2001, **73**, 121–136.
20 R. Sinha, G. J. Kim, S. Nie and D. M. Shin, *Mol. Cancer Ther.*, 2006, **5**, 1909–1917.
21 R. Cheng, F. Meng, C. Deng, H.-A. Klok and Z. Zhong, *Biomaterials*, 2013, **34**, 3647–3657.
22 J. E. Lewis, E. L. Gavey, S. A. Cameron and J. D. Crowley, *Chem. Sci.*, 2012, **3**, 778–784.
23 V. P. Torchilin, *Nat. Rev. Drug Discovery*, 2014, **13**, 813–827.
24 C. F. Anderson and H. Cui, *Ind. Eng. Chem. Res.*, 2017, **56**, 5761–5777.
25 C. Alvarez-Lorenzo, L. Bromberg and A. Concheiro, *Photochem. Photobiol.*, 2009, **85**, 848–860.
26 D. Schmaljohann, *Adv. Drug Delivery Rev.*, 2006, **58**, 1655–1670.
27 N. K. Singh and D. S. Lee, *J. Controlled Release*, 2014, **193**, 214–227.
28 Z. Zhao, H. Meng, N. Wang, M. J. Donovan, T. Fu, M. You, Z. Chen, X. Zhang and W. Tan, *Angew. Chem.*, 2013, **52**, 7487–7491.
29 Y. Zhang, J. W. Chan, A. Moretti and K. E. Uhrich, *J. Controlled Release*, 2015, **219**, 355–368.
30 J. Croissant, X. Cattoën, M. W. C. Man, A. Gallud, L. Raehm, P. Trens, M. Maynadier and J. O. Durand, *Adv. Mater.*, 2014, **26**, 6174–6180.
31 Q. Pei, X. Hu, J. Zhou, S. Liu and Z. Xie, *Biomater. Sci.*, 2017, **5**, 1517–1521.
32 D. Yang, W. Chen and J. Hu, *J. Phys. Chem. B*, 2014, **118**, 12311–12317.
33 Q. Zhang, J. He, M. Zhang and P. Ni, *J. Mater. Chem. B*, 2015, **3**, 4922–4932.
34 M. Wang, J. Yan, C. Li, X. Wang, J. Xiong, D. Pan, L. Wang, Y. Xu, X. Li and M. Yang, *Eur. Polym. J.*, 2020, **123**, 109462.
35 L. Lu, B. Li, C. Lin, K. Li, G. Liu, Z. Xia, Z. Luo and K. Cai, *J. Mater. Chem. B*, 2020, **8**, 3918–3928.
36 J. E. Biaglow and R. A. Miller, *Cancer Biol. Ther.*, 2005, **4**, 13–20.
37 J. M. Estrela, A. Ortega and E. Obrador, *Crit. Rev. Clin. Lab. Sci.*, 2006, **43**, 143–181.
38 A. Russo, W. DeGraff, N. Friedman and J. B. Mitchell, *Cancer Res.*, 1986, **46**, 2845.
39 D. Y.-K. Wong, Y.-L. Hsiao, C.-K. Poon, P.-C. Kwan, S.-Y. Chao, S.-T. Chou and C.-S. Yang, *Cancer Lett.*, 1994, **81**, 111–116.
40 R. B. Greenwald, A. Pendri, C. D. Conover, C. Lee, Y. H. Choe, C. Gilbert, A. Martinez, J. Xia, D. C. Wu and M. Hsue, *Bioorg. Med. Chem.*, 1998, **6**, 551–562.
41 J. D. Hartgerink, E. Beniash and S. I. Stupp, *Science*, 2001, **294**, 1684–1688.
42 H. Y. Wen, H. Q. Dong, W. J. Xie, Y. Y. Li, K. Wang, G. M. Pauletti and D. L. Shi, *Chem. Commun.*, 2011, **47**, 3550–3552.
43 A. Safavy, G. I. Georg, D. Vander Velde, K. P. Raisch, K. Safavy, M. Carpenter, W. Wang, J. A. Bonner, M. B. Khazaeli and D. J. Buchsbaum, *Bioconjugate Chem.*, 2004, **15**, 1264–1274.
44 H. Dong, S. E. Paramonov, L. Aulisa, E. L. Bakota and J. D. Hartgerink, *J. Am. Chem. Soc.*, 2007, **129**, 12468–12472.
45 F. Wurthner, T. E. Kaiser and C. R. Saha-Moller, *Angew. Chem., Int. Ed.*, 2011, **50**, 3376–3410.
46 T. Miyazawa and E. R. Blout, *J. Am. Chem. Soc.*, 1961, **83**, 712–719.
47 G. W. M. Vandermeulen, K. T. Kim, Z. Wang and I. Manners, *Biomacromolecules*, 2006, **7**, 1005–1010.
48 W. Y. Seow, G. Salgado, E. B. Lane and C. A. Hauser, *Sci. Rep.*, 2016, **6**, 32670.
49 G. L. Ellman, *Arch. Biochem. Biophys.*, 1959, **82**, 70–77.
50 A. Singh, S. Boldin-Adamsky, R. K. Thimmulappa, S. K. Rath, H. Ashush, J. Coulter, A. Blackford, S. N. Goodman, F. Bunz and W. H. Watson, *Cancer Res.*, 2008, **68**, 7975–7984.
51 A. Singh, V. Misra, R. K. Thimmulappa, H. Lee, S. Ames, M. O. Hoque, J. G. Herman, S. B. Baylin, D. Sidransky and E. Gabrielson, *PLoS Med.*, 2006, **3**, e420.

 This journal is © The Royal Society of Chemistry 2020